# A Topological Investigation of Power Flow

Hale Cetinay, Fernando A. Kuipers, *Senior Member, IEEE*, and Piet Van Mieghem

***Abstract*—This paper combines the fundamentals of an electrical grid, such as flow allocation according to Kirchhoff's laws and the effect of transmission line reactances with spectral graph theory, and expresses the linearized power flow behaviour in slack-bus independent weighted graph matrices to assess the relation between the topological structure and the physical behaviour of a power grid. Based on the pseudoinverse of the weighted network Laplacian, the paper further analytically calculates the effective resistance (Thevenin) matrix and the sensitivities of active power flows to the changes in network topology by means of transmission line removal and addition. Numerical results for the IEEE 118-bus power system are demonstrated to identify the critical components to cascading failures, node isolation, and Braess' paradox in a power grid.**

***Index Terms*—Complex networks, load flow, network topology, power grids, sensitivity analysis.**

## I. Introduction

THE unavailability of electrical power can severely disrupt daily life and result in substantial economic and social costs [1]. This key importance of electrical power supply encourages a robust design and a careful operation of the electrical grid [2]. Electrical grid operators need to assess power system security in order to find and analyze the system's critical components during regular operations, but also in the event of component failure or when planning to add new components.

The topology of power grids is a complex network [3], [4]. This observation has opened the door to a new direction in studying power system vulnerabilities, namely, a complex networks perspective [5], [6]. A significant part of such complex network studies investigate the relationship between the topology and specific performance metrics for power grids [5], [7], [8]. Various metrics [9] are proposed to assess the vulnerability of the power grid [5], [10], [11], and to identify its critical network elements [12], [13]. Most of these studies are based on classical topology metrics (such as nodal degree, clustering coefficient [10], [11]), which ignore the electrical properties, such as flow allocation according to Kirchhoff's laws or the impedance values of transmissions lines in the grid.

Two different aspects are important in the distribution of power flows, and consequent system vulnerability, in an electrical grid: the operating state, including the generator and load dispatches of the system, and the topology of the network formed by electrical buses and their interconnection. Accordingly, some studies propose extended topological metrics (such as effective graph resistance and net-ability [8], [12], [14]) that reflect some of the electrical properties of grids, and some studies introduce combined topological and operational algorithms to identify critical lines [15]. Through empirical studies, those metrics, based on effective resistance, have shown to perform better in assessing the vulnerability of power grids than purely topological approaches. Motivated by this fact and results from empirical studies with extended graph metrics, this paper presents an analytical approach to the distribution of flows in power grids that directly captures the impact of the topological structure on those flows. A slack-bus independent representation, in full-rank topology matrices, of power flow behaviour is introduced. Additionally, a closed-form expression for the effective resistance (Thevenin) matrix that represents the topology as well as the power flow allocation behaviour, is derived. Those formulae allow the computation of the redistribution of power flows under network topology changes, and they provide a more fine-grained analysis of the critical elements in power grids.

The work presented here only makes one approximation: the linearization of the power flow equations resulting in the so-called dc flow equations [16], which facilitates the use of enhanced linear algebra and graph theory leading to expressions that may simplify the design of robust power grids. In particular, the contributions of this paper are as follows: 1) a slack-bus independent expression for the linearized power flow; 2) an analytical derivation of the effective resistance (Thevenin) matrix of a power grid; and 3) expressions for the pseudoinverse of the network Laplacian and the redistribution of the power flow under link removal/addition.

The remainder of this paper is organized as follows. Section II provides a spectral graph perspective [17] to the linearized power flow equations and calculates the effective resistance matrix [18] in power grids. Section III develops expressions for the pseudoinverse of the weighted Laplacian and the sensitivities of active power flows under link removal/addition. Section IV illustrates the proposed formulations and Section V concludes the paper.

## II. Spectral Decomposition in Power Flow Equations

This section introduces a spectral graph perspective [17] to the linearized power flow equations and applies the concept of the effective resistance [18] to power grids.

### A. Solution of Power Flow Equations

A power grid with $N$ buses, and $L$ transmission lines and transformers is a complex network, whose underlying topology

Manuscript received January 15, 2016; revised April 8, 2016; accepted May 17, 2016. Date of publication July 7, 2016; date of current version August 23, 2018. This work was supported by Alliander N.V.

The authors are with the Faculty of Electrical Engineering, Mathematics and Computer Science, Delft University of Technology, Delft 2600 GA, The Netherlands (e-mail: H.Cetinay-Iyicil@tudelft.nl; F.A.Kuipers@tudelft.nl; P.F.A.VanMieghem@tudelft.nl).

Digital Object Identifier 10.1109/JSYST.2016.2573851

can be represented by a graph $G(\mathcal{N},\mathcal{L})$, where $\mathcal{N}$ denotes the set of $N$ nodes and $\mathcal{L}$ denotes the set of $L$ links. The $N\times N$ adjacency matrix $\mathbf{A}$ specifies the interconnection pattern of the graph $G(\mathcal{N},\mathcal{L})$: $a_{ik}=1$ only if the pair of nodes $i$ and $k$ are connected by a link; otherwise $a_{ik}=0$. The nonlinear power flow dynamics can be approximated by a set of linear equations (38) given in the Appendix assuming dc load flow [16], [19]. Consequently, the dc flow equations of the electrical network can be written in terms of the adjacency matrix of $G(\mathcal{N},\mathcal{L})$:

$$p_i=\sum_{k=1}^{N}a_{ik}b_{ik}(\theta_i-\theta_k)=\theta_i\sum_{k=1}^{N}a_{ik}b_{ik}-\sum_{k=1}^{N}a_{ik}b_{ik}\theta_k \quad (1)$$

where $b_{ik}$ is reciprocal of transmission line reactance between the buses $i$ and $k$, $p_i$ is the active power injected at bus $i$, and $\theta_i$ and $\theta_k$ are the voltage phase angles at bus $i$ and bus $k$, respectively.[1]

The effects of line reactances are represented by the weighted adjacency matrix $\mathbf{W}$, where each element $w_{ik}=a_{ik}b_{ik}$ is the weight of the link between nodes[2] $i$ and $k$:

$$p_i=\theta_i\sum_{k=1}^{N}w_{ik}-\sum_{k=1}^{N}w_{ik}\theta_k. \quad (2)$$

Since (2) holds for every bus $i$ in the electrical network, the corresponding matrix representation is

$$\begin{aligned}\mathbf{P}&=\left\{\mathbf{diag}\left(\sum_{k=1}^{N}w_{ik}\right)-\mathbf{W}\right\}\boldsymbol{\Theta}\\&=(\mathbf{D}-\mathbf{W})\boldsymbol{\Theta}\end{aligned} \quad (3)$$

where $\mathbf{P}=[p_1\ldots p_N]^{\mathrm{T}}$ is the vector of net active power injection at the nodes,[3] $\mathbf{D}$ is the weighted degree diagonal matrix, and $\boldsymbol{\Theta}=[\theta_1\ldots\theta_N]^{\mathrm{T}}$ is the vector of voltage phase angles. Finally, introducing the weighted Laplacian $\tilde{\mathbf{Q}}=\mathbf{D}-\mathbf{W}$ into (3) yields

$$\mathbf{P}=\tilde{\mathbf{Q}}\boldsymbol{\Theta} \quad (4)$$

where the weighted Laplacian is a symmetric, positive semidefinite matrix that possesses nonnegative eigenvalues apart from the smallest eigenvalue, which is zero [17].

The solution to the dc power flow equation requires finding unknown voltage phase angles at each node in the network for the given generation and load profiles. Due to the zero eigenvalue of $\tilde{\mathbf{Q}}$, the matrix equation in (4) cannot be inverted. However, using spectral decomposition [17], any real and symmetric matrix can be written as $\tilde{\mathbf{Q}}=\mathbf{X}\boldsymbol{\Lambda}\mathbf{X}^{\mathbf{T}}$, where $\boldsymbol{\Lambda}=\mathbf{diag}(\mu_j)_{1\le j\le N}$ and $\mathbf{X}=[\mathbf{x_1}\ldots\mathbf{x_N}]$ is an orthogonal matrix formed by the eigenvectors $\mathbf{x_1},\ldots,\mathbf{x_N}$ of $\tilde{\mathbf{Q}}$ corresponding to the eigenvalues $\mu_1\ge\mu_2\ge\ldots\ge\mu_N=0$. The eigenvector $\mathbf{x_j}$ is normalized as $\mathbf{x_j}^{\mathbf{T}}\mathbf{x_j}=1$. Then, expanding $\tilde{\mathbf{Q}}$

$$\tilde{\mathbf{Q}}=\sum_{j=1}^{N}\mu_j\mathbf{x_j}\mathbf{x_j^T}=\sum_{j=1}^{N-1}\mu_j\mathbf{x_j}\mathbf{x_j^T}+\frac{\mu_N}{N}\mathbf{u}\mathbf{u}^{\mathbf{T}}=\sum_{j=1}^{N-1}\mu_j\mathbf{x_j}\mathbf{x_j^T} \quad (5)$$

where $\mathbf{u}$ is the all-one vector, shows that the last equation corresponding to $\mu_N=0$ can be omitted. Proceeding with the symmetric $N\times N$ matrix $\hat{\mathbf{Q}}=\hat{\mathbf{X}}\mathrm{diag}(\mu_k)\hat{\mathbf{X}}^{\mathbf{T}}$, where the $N\times(N-1)$ matrix $\hat{\mathbf{X}}$ consists of all the eigenvectors of $\tilde{\mathbf{Q}}$ except the eigenvector $\mathbf{u}$ belonging to $\mu_N=0$, and where the $(N-1)\times(N-1)$ diagonal matrix $\mathbf{diag}(\mu_k)$ contains the positive eigenvalues of $\tilde{\mathbf{Q}}$, the inverse of $\hat{\mathbf{Q}}$ can be found as

$$\hat{\mathbf{Q}}^{-\mathbf{1}}=(\sum_{k=1}^{N-1}\mu_k\mathbf{x_k}\mathbf{x_k^T})^{-1}=\sum_{k=1}^{N-1}\frac{1}{\mu_k}\mathbf{x_k}\mathbf{x_k^T}=\tilde{\mathbf{Q}}^{+} \quad (6)$$

where the $N\times N$ matrix $\tilde{\mathbf{Q}}^{+}=\hat{\mathbf{X}}\mathbf{diag}(\mu_k^{-1})\hat{\mathbf{X}}^{\mathbf{T}}$ is the pseudoinverse of the Laplacian obeying

$$\begin{aligned}\tilde{\mathbf{Q}}^{+}\tilde{\mathbf{Q}}&=\sum_{k=1}^{N-1}\frac{1}{\mu_k}\mathbf{x_k}\mathbf{x_k^T}\sum_{j=1}^{N-1}\mu_j\mathbf{x_j}\mathbf{x_j^T}\\&=\sum_{k=1}^{N-1}\sum_{j=1}^{N-1}\mu_j\frac{1}{\mu_k}\mathbf{x_k}(\mathbf{x_k^T}\mathbf{x_j})\mathbf{x_j^T}\\&=\mathbf{I}-\frac{1}{N}\mathbf{J}\end{aligned} \quad (7)$$

where $\mathbf{I}$ is the identity matrix and $\mathbf{J}$ the all-one matrix.

Using $\tilde{\mathbf{Q}}^{+}$, the pseudoinversion of (4) gives

$$\boldsymbol{\Theta}=\tilde{\mathbf{Q}}^{+}\mathbf{P}. \quad (8)$$

Equation (8) physically means that only the differences of voltage phase angles between the network buses matter for the power flow. Additionally, an average value of 0 has been chosen as reference for the node voltage phase angles and, consequently, the concept of slack-bus [20] becomes redundant, as a reference is already included in the graph matrix representation.

The active power flow $f_{ik}$ over the link between nodes $i$ and $k$ can be calculated using the dc load flow assumptions given in the Appendix:

$$f_{ik}=b_{ik}(\theta_i-\theta_k). \quad (9)$$

As (9) holds for every link, the corresponding matrix equation is

$$\mathbf{F}=\tilde{\mathbf{B}}^{\mathbf{T}}\boldsymbol{\Theta} \quad (10)$$

where the $L\times 1$ vector $\mathbf{F}=[f_1\ldots f_L]^{\mathrm{T}}$ is the active power flow over the network links and $\tilde{\mathbf{B}}$ is the $N\times L$ weighted incidence matrix of the graph with the elements

$$\tilde{b}_{il}=\begin{cases}w_{ik} & \text{if link } e_l=i\to k\\ -w_{ik} & \text{if link } e_l=\ i\leftarrow k\\ 0 & \text{otherwise.}\end{cases} \quad (11)$$

Combining (8) and (10) results in the final equation for the active power flows over the graph links:

$$\mathbf{F}=\tilde{\mathbf{B}}^{\mathbf{T}}\tilde{\mathbf{Q}}^{+}\mathbf{P}. \quad (12)$$

[1]Matrices are written in bold and their components are in lower case.

[2]Parallel links connecting the same pair of nodes are replaced by a single link with equivalent reactance calculated from Ohm's law.

[3]A balanced dc power flow is assumed, i.e., $\mathbf{u}^{\mathrm{T}}\mathbf{P}=0$.

The above equation represents, assuming that the dc load flow equation is sufficiently accurate, the relation between the active power flows over the network links for the given generation and load profile $\mathbf{P}$, and the graph-related matrices $\tilde{\mathbf{B}}$ and $\tilde{\mathbf{Q}}$.

### B. Calculation of the Effective Resistance Matrix

In graph theory, the resistance distance between a pair of nodes is the potential difference between those two nodes in an electrical network, when a unit current is injected at one node and leaves the network at the other node [18], [21]. In a power grid, there are generator and load buses and, under dc load flow assumptions, active power flows over the network lines resulting in voltage phase angle differences. This analogy enables the introduction of the concept of the effective resistance matrix $\mathbf{\Omega}$ with the elements $\omega_{ab}$ to capture the relation between the voltage phase angle and injected active power:

$$\theta_a - \theta_b = \omega_{ab}\, p_{ab} \tag{13}$$

where $a$ is a source node (generator bus), $b$ is a sink node (load bus), $p_{ab}$ is the active power injected into the network at node $a$ and leaving from node $b$, and $\theta_a$ and $\theta_b$ are the voltage phase angles at nodes $a$ and $b$, respectively.

Introducing (8) into (13) gives

$$(\mathbf{e_a} - \mathbf{e_b})^{\mathrm{T}} \mathbf{\Theta} = (\mathbf{e_a} - \mathbf{e_b})^{\mathrm{T}} \tilde{\mathbf{Q}}^{+} p_{ab} (\mathbf{e_a} - \mathbf{e_b}) \tag{14}$$

where $\mathbf{e_k}$ is the basic vector with the $m$th component equal to 1 if $m = k$, else 0, and the effective resistance or Thevenin resistance $\omega_{ab}$ between nodes $a$ and $b$ can be expressed as

$$\omega_{ab} = (\mathbf{e_a} - \mathbf{e_b})^{\mathrm{T}} \tilde{\mathbf{Q}}^{+} (\mathbf{e_a} - \mathbf{e_b}). \tag{15}$$

Multiplying out the right-hand side of (15) yields

$$\omega_{ab} = (\tilde{\mathbf{Q}}^{+})_{aa} + (\tilde{\mathbf{Q}}^{+})_{bb} - 2(\tilde{\mathbf{Q}}^{+})_{ab} \tag{16}$$

from which the symmetric effective resistance matrix $\mathbf{\Omega}$ of the electrical power network can be calculated as

$$\mathbf{\Omega} = \mathbf{z}\mathbf{u}^{\mathbf{T}} + \mathbf{u}\mathbf{z}^{\mathbf{T}} - 2\tilde{\mathbf{Q}}^{+} \tag{17}$$

where the vector $\mathbf{z} = [(\tilde{\mathbf{Q}}^{+})_{11} (\tilde{\mathbf{Q}}^{+})_{22} \ldots (\tilde{\mathbf{Q}}^{+})_{NN})]^{\mathrm{T}}$.

The effective resistance matrix allows to introduce the concept of electrical flow distance rather than physical distances or link weights in the graph. A strong electrical connection between a pair of nodes results in a low effective resistance [12].

## III. Impact of Topology on Power Flows

As shown so far, the electrical flow depends on the network topology as well as on the power input. In this section, effective resistances will be used to capture the flow distribution under the changes in network topology.

### A. Link Removal

An electrical grid is expected to tolerate the loss of any single component at any time (which is called the $N-1$ criterion [2]). Due to the loss of a network component, the power in the electrical grid will be redistributed, and the resulting situation can lead to an increase or a decrease in power flow over a particular network link. The link removal that causes intolerable increases in the power flow needs to be carefully studied and necessary measures should be taken to avoid cascading failures [12].

Existing flow-based studies require the solution of system equations for each contingency under each loading scenario. Thus, computationally effective alternatives are needed, and power transfer (PTDF) and line outage (LODF) distribution factors are often used [22]–[24]. These metrics capture the relative change in power flow over a particular link, after a change in injection and corresponding withdrawal at a pair of nodes (PTDF) or after link outages (LODF). LODF is calculated once for each link removal by solving the flow equations for an arbitrary power input, and can be used for each loading scenario using linearity. These direct calculations decrease the computation time, yet it is not possible to reflect the drivers of flow behaviour as the formulations are result-oriented and based on reduced matrices in the absence of the slack-bus(es). On the contrary, in this section, link removals in a power grid are analyzed topologically in order to investigate the influence of effective resistances and link weights.

When an arbitrary transmission link $l_{ij}$ in an electrical grid is removed, the network topology is changed. Following the definition of weighted adjacency matrix in Section II-A, the removal of the link between the nodes $i$ and $j$ zeroes the entries $w_{ij}$ and $w_{ji}$ in the new weighted adjacency matrix, whereas the other elements remain unchanged. As a result, the Laplacian of the network will be affected in the $i$th and $j$th rows by the weight of the removed link on the diagonal entry and $j$th and $i$th columns, respectively. The relation between the two Laplacians is essentially a rank-one update:

$$\tilde{\mathbf{Q}}' = \tilde{\mathbf{Q}} - w_{ij}(\mathbf{e_i} - \mathbf{e_j})(\mathbf{e_i} - \mathbf{e_j})^{\mathrm{T}} \tag{18}$$

where $\tilde{\mathbf{Q}}$ is the initial Laplacian of the network, $\tilde{\mathbf{Q}}'$ is the Laplacian of the network after the removal of link $l_{ij}$, and $w_{ij}$ is the weight of the link. Introducing Meyer's relation [25] between the pseudoinverses denoted by $^{+}$

$$(\mathbf{A} + \mathbf{c}\mathbf{d}^{\mathbf{T}})^{+} = \mathbf{A}^{+} - (1 + \mathbf{d}^{\mathbf{T}}\mathbf{A}^{+}\mathbf{c})^{-1}\mathbf{A}^{+}\mathbf{c}\mathbf{d}^{\mathbf{T}}\mathbf{A}^{+} \tag{19}$$

allows to express the pseudoinverse $\hat{\mathbf{Q}}'^{+}$ of the new Laplacian in (18) in terms of the initial pseudoinverse $\hat{\mathbf{Q}}^{+}$ and effective resistances in (15) as

$$\begin{aligned}\tilde{\mathbf{Q}}'^{+} &= (\tilde{\mathbf{Q}} + (-w_{ij})(\mathbf{e_i} - \mathbf{e_j})(\mathbf{e_i} - \mathbf{e_j})^{\mathrm{T}})^{+} \\ &= \hat{\mathbf{Q}}^{+} + \frac{w_{ij}}{1 - w_{ij}\omega_{ij}} \hat{\mathbf{Q}}^{+}(\mathbf{e_i} - \mathbf{e_j})(\mathbf{e_i} - \mathbf{e_j})^{\mathrm{T}} \hat{\mathbf{Q}}^{+}\end{aligned} \tag{20}$$

where $\omega_{ij}$ is the effective resistance between nodes $i$ and $j$.

When link $l_{ij}$ is removed, the active power flow $f_{ij}$ over the link before removal is redistributed over alternative paths between nodes $i$ and $j$. Under the dc flow approximation, which results in (12) being linear, the redistribution can be perceived as an additional injection of active power $f_{ij}$ at node $i$ and leaving node $j$ in the new network, provided that the load and generation profiles of the grid $\mathbf{P}$ remain unchanged. Hence, the final active power flow over an arbitrary link $l_{ab}$ can be written as the sum of the previous state of the system, i.e., the previous flow over the link between nodes $a$ and $b$ when link $l_{ij}$ is present, and the flow resulting from the change of the state due to link

removal. Consequently, the change of the active power flow over the observed link $l_{ab}$ can be calculated using (12) as

$$\Delta f_{ab} = w_{ab} \times (\mathbf{e_a} - \mathbf{e_b})^{\mathrm{T}} \tilde{\mathbf{Q}}'^{+} (\mathbf{e_i} - \mathbf{e_j}) \times f_{ij} \tag{21}$$

where $\Delta f_{ab}$ is the change in the active power flow over link $l_{ab}$ due to removal of link $l_{ij}$, and $w_{ab}$ is the weight of link $l_{ab}$. Inserting (20) into (21) results in

$$\begin{aligned}\Delta f_{ab} &= f_{ij} \times w_{ab} (\mathbf{e_a} - \mathbf{e_b})^{\mathrm{T}} \tilde{\mathbf{Q}}'^{+} (\mathbf{e_i} - \mathbf{e_j}) \\ &= f_{ij} \times w_{ab} \left(1 + \frac{\omega_{ij} w_{ij}}{1 - w_{ij}\omega_{ij}}\right) (\mathbf{e_a} - \mathbf{e_b})^{\mathrm{T}} \hat{\mathbf{Q}}^{+} (\mathbf{e_i} - \mathbf{e_j}).\end{aligned} \tag{22}$$

As $(\mathbf{e_a} - \mathbf{e_b})^{\mathrm{T}} \hat{\mathbf{Q}}^{+} (\mathbf{e_i} - \mathbf{e_j}) = \frac{1}{2}(\omega_{aj} - \omega_{ai} + \omega_{bi} - \omega_{bj})$ according to (16), we have

$$\Delta f_{ab} = f_{ij} \times w_{ab} \times \frac{\omega_{aj} - \omega_{ai} + \omega_{bi} - \omega_{bj}}{2(1 - w_{ij}\omega_{ij})}$$

or

$$\frac{\Delta f_{ab}}{f_{ij}} = w_{ab} \times \frac{\omega_{aj} - \omega_{ai} + \omega_{bi} - \omega_{bj}}{2(1 - w_{ij}\omega_{ij})}. \tag{23}$$

Equation (23) shows that, due to the removal of link $l_{ij}$, the resultant change in the active power over a remaining link $l_{ab}$ is determined by the network topology via the effective resistances between the node pairs, and the previous flow $f_{ij}$ over the removed link. Several observations follow from (23).

1) The resulting change $\Delta f_{ab}$ in active power flow over a link $l_{ab}$ depends on and is limited by the magnitude of the previous flow $f_{ij}$ over the removed link $l_{ij}$. Indeed, since the active power is redistributed over the network, it holds that $\left|\frac{\Delta f_{ab}}{f_{ij}}\right| \leq 1$, which forces the right-hand side of (23) to be between $-1$ and 1.
2) If the directions of the links are defined to be the same as the direction of the initial flow over the links, a positive (negative) number in the right-hand side of (23) indicates an increase (decrease) in the active power flow over the remaining link in that direction.
3) From a robustness point of view, the network links whose removal sharply increases the active power flow over the remaining links are critical. In addition, the network links that are severely affected by different link removal scenarios are also critical.
4) For the network links whose active power flows are not affected by the removal, the right-hand side of (23) must be 0, meaning the equality $\omega_{aj} + \omega_{bi} = \omega_{ai} + \omega_{bj}$ between the effective resistances of node pairs is satisfied. This equality is satisfied for the links that are in branches[4] of the network and for Wheatstone bridges [26] if they are present in the network.
5) The denominator $(1 - w_{ij}\omega_{ij})$ of (23) is zero when the electrical distance between the nodes of the link is equal to the inverse of the link weight, i.e., line reactance. It shows that there is no alternative parallel (back-up) path in the network for the removed link. Therefore, when this link is removed, some nodes in the network will be isolated and the power flow cannot be redistributed without the change of generation and load profiles. In such a case, (23) can be rewritten as

$$\frac{\Delta f_{ab}}{f_{ij}} = \begin{cases} \text{Network islanded (N.I.),} & \text{if } w_{ij} \times \omega_{ij} = 1 \\ w_{ab} \times \dfrac{\omega_{aj} - \omega_{ai} + \omega_{bi} - \omega_{bj}}{2(1 - w_{ij}\omega_{ij})}, & \text{otherwise.} \end{cases} \tag{24}$$

Equation (24) captures the final network status, i.e., islanded or not, as well as the effect of link removal on the distribution of flows over the remaining network links, when the network is not partitioned. The calculation is based on the initial graph-related matrices, and the computation of new topological matrices is avoided. Consequently, by spectral decomposition, once the effective resistance matrix is calculated, the effect of any link removal can be calculated from (24) for any loading scenario.

### *B. Link Addition*

The overloads in the transmission lines of a power grid can be solved by generation/load shifting in the short term. However, a long-term investment (such as addition of new transmission lines) needs to be planned in the case of persistent overloads or to satisfy the $N - 1$ criterion [2].

Determining the right location of a new link is challenging. It is desirable that the added link increases the robustness of the power grid by decreasing the critical flows over the network links. In flow-based studies, the computational complexity is high, thus alternatives which decrease the calculation time and determine the right investment for the system are sought [8], as provided in this section.

It is assumed that a new link can be added between any arbitrary two nodes (connected or unconnected) $i$ and $j$ in the electrical grid. Similar to Section III-A, the redistribution of flows due to link addition can be perceived in the initial network as an additional injection of the active power $f_{ij}$ over the new link at node $j$ and leaving from node $i$, i.e., in the opposite direction of the new flow. The change in the power flow $\Delta f_{ab}$ over an arbitrary network link $l_{ab}$ under the dc power flow approximation is calculated as

$$\Delta f_{ab} = w_{ab} (\mathbf{e_a} - \mathbf{e_b})^{\mathrm{T}} \tilde{\mathbf{Q}}^{+} (\mathbf{e_i} - \mathbf{e_j}) \times (-f_{ij})$$

and, using (16), as

$$\frac{\Delta f_{ab}}{f_{ij}} = \frac{w_{ab}(\omega_{ai} - \omega_{aj} + \omega_{bj} - \omega_{bi})}{2} \tag{25}$$

where the flow $f_{ij}$ over the new link is calculated by using the new pseudoinverse $\tilde{\mathbf{Q}}'^{+}$ of the Laplacian and the power input $\mathbf{P}$ of the network:

$$f_{ij} = w_{ij} (\mathbf{e_i} - \mathbf{e_j})^{\mathrm{T}} \tilde{\mathbf{Q}}'^{+} \mathbf{P}. \tag{26}$$

The addition of the link changes the Laplacian of the network and the relation between the new $\tilde{\mathbf{Q}}'^{+}$ and the old Laplacian

[4]Here, branches of a network refer to the network links that are connected radially to the meshed part of the network.

$\tilde{\mathbf{Q}}^{+}$ becomes

$$\tilde{\mathbf{Q}}' = \tilde{\mathbf{Q}} + (w_{ij})(\mathbf{e_i} - \mathbf{e_j})(\mathbf{e_i} - \mathbf{e_j})^{\mathrm{T}}. \tag{27}$$

Relation (19) shows that the new pseudoinverse can be represented as

$$\begin{aligned}\tilde{\mathbf{Q}}'^{+} &= (\tilde{\mathbf{Q}} + (w_{ij})(\mathbf{e_i} - \mathbf{e_j})(\mathbf{e_i} - \mathbf{e_j})^{\mathrm{T}})^{+} \\ &= \hat{\mathbf{Q}}^{+} - \frac{w_{ij}}{1 + w_{ij}\omega_{ij}}\, \hat{\mathbf{Q}}^{+}(\mathbf{e_i} - \mathbf{e_j})(\mathbf{e_i} - \mathbf{e_j})^{\mathrm{T}} \hat{\mathbf{Q}}^{+}. \end{aligned} \tag{28}$$

Using the above derivation (28) of the new pseudoinverse $\tilde{\mathbf{Q}}'^{+}$, (26) can be rewritten as

$$f_{ij} = \frac{w_{ij}}{1 + w_{ij}\omega_{ij}} \times \theta_{ij}. \tag{29}$$

Equation (29) shows that the new flow $f_{ij}$ over the added link $l_{ij}$ is related to the previous network conditions, i.e., the difference between the voltage phase angles at nodes $i$ and $j$, and inversely related to the effective resistance between these nodes. As $\theta_{ij}$ and $\omega_{ij}$ are fixed by the initial network topology, the maximum flow over the added link $\frac{|\theta_{ij}|}{\omega_{ij}}$ is achieved when the link weight $w_{ij}$ tends to infinity, meaning that the reactance of the transmission line is close to zero, a short circuit of the nodes. Conversely, the flow over the new link is minimum, 0, when $w_{ij}$ approaches zero, meaning connecting an infinite reactance between the nodes (an open circuit). Then, by adjusting the link weight $w_{ij}$ through reconducting or replacing the conductors, it is theoretically possible to adjust the magnitude of the flow over the added link.

The term $\frac{w_{ij}}{1+w_{ij}\omega_{ij}}$ in the right-hand side of (29) is strictly positive for passive network elements. Thus, the direction of the active power flow over the new link is determined only by the difference between the phase angles of voltage $\theta_{ij}$ in the initial network. A positive difference in voltage phase angles $\theta_{ij}$ results in an active power flow from node $i$ to node $j$, when the nodes are connected by a link, whereas the opposite results in a flow from node $j$ to node $i$. If the voltage phase angle difference $\theta_{ij}$ is zero, there will be no power flow over the link when these nodes are connected by a link (Wheatstone bridge [26]).

Inserting the result (29) of the flow over the new link into (25), the change in the active power flow over the observed link $l_{ab}$ due to link addition can be calculated as

$$\Delta f_{ab} = \frac{w_{ab}w_{ij}(\omega_{ai} - \omega_{aj} + \omega_{bj} - \omega_{bi})}{2(1 + w_{ij}\omega_{ij})} \times \theta_{ij}. \tag{30}$$

Equation (30) shows that the change $\Delta f_{ab}$ in the flow over the network links is determined by the network topology via the effective resistances and initial network conditions, whereas the relative change to the flow $f_{ij}$ over the new link in (25) depends only on the network topology. Observations from (25) and (30) are as follows.

1) The change in the active power flow over network links depends linearly on the flow over the added link and the changes in active power flows over the initial network links are bounded by this value. When the right-hand side of (25) is 1 or $-1$, it means that the flow over the observed link is directly affected by the link addition.
2) The numerator of (25) is zero when the equality between the effective resistances $\omega_{ai} - \omega_{aj} = \omega_{bi} - \omega_{bj}$ is satisfied, meaning the added link has no effect on the active power flow over the observed network link. This is possible for the observed/added links that are in branches.
3) If the direction of the link is defined as the direction of the initial flow over that link, then a positive (negative) number in the right-hand side of (30) corresponds to an increase (decrease) in the active power flow over the observed link in that direction. Clearly, a decrease in the flow over all network lines is desired.

Finally, (23) and (25) show that the effective resistances between the node pairs of the observed and the removed/added links determine the effect on the flow over the observed link. This aligns with the empirical studies that capture the relation between the effective graph resistance value [18] and the robustness of the power grid against cascading failures [8], [12]. Additionally, the weight of the observed link $w_{ab}$ is found to be influential in both link removal and addition calculations, whereas the weight of the added link $w_{ij}$ does not affect the flow over the observed link relative to the flow over the added link.

From the graph-related matrices, the changes (23) and (25) in the active power flow over the network links relative to flow over the removed/added link can be represented. However, for the magnitude of the change, initial conditions, the generation and load profiles of the network, must be known. The direction of the change in the flow over the observed link, i.e., decrease or increase in magnitude, is also determined by both the network topology and the power input of the electrical network as it depends on the existing flow and its direction. However, in electrical grids with limited generation and load variations, such as directed distribution networks, it is possible to know the flow directions in advance. Therefore, from the effective resistances, the relative effect on the magnitude can be found. For the meshed networks with various generation and load dispatches, such as high-voltage transmission networks, the flow directions may be unknown. Therefore, initial network conditions, the voltage phase angles, or the power input of the network must be used in the calculations regarding the direction.

## IV. Numerical Analysis

This section demonstrates the results derived in Section III. For ease of inspection, first a quantitative analysis is performed for a small test network. Later, the analysis is demonstrated for the IEEE 118-bus power system.[5]

### A. Synthetic Example

The network in Fig. 1(a) contains six nodes and seven links. For simplicity, link weights, the reciprocal of transmission line reactances are set to unity. The direction of the existing flows over the links is defined to be always from lower to higher node index. The effective resistance matrix $\boldsymbol{\Omega}$ is calculated according to (17) and the effective resistances are shown in Fig. 1(b). The minimum effective resistance is between nodes 2 and 4,

[5]IEEE 118-Bus Power Flow Test Case. [Online]. Available: http://www.ee.washington.edu/research/pstca/

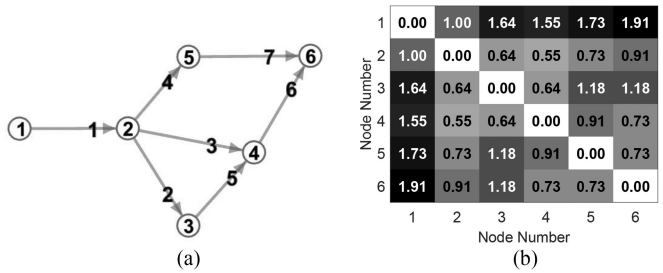


Fig. 1. Test network. (a) Graph, and (b) Effective resistances.

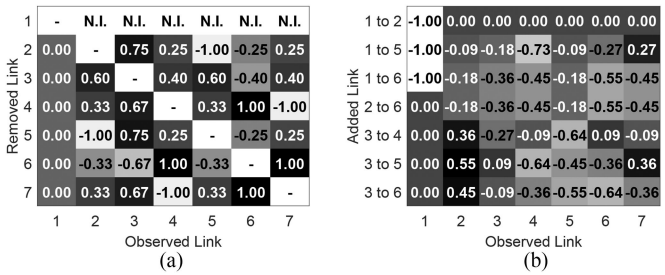


Fig. 2. Effect of link removal and addition, $\frac{\Delta f_{ab}}{f_{ij}}$. (a) Link removal, and (b) Link addition.

whereas the largest is between nodes 1 and 6. The definition of electrical distance in (13) shows that the highest difference in the voltage phase angles of the network nodes occurs when the electrical power is transferred between those nodes, leading to larger flows over the network links from (9). Conversely, the minimum difference in the angles of the voltage phasors of the network nodes occurs for the same amount of electrical power when it is transferred between nodes 2 and 4, leading to smaller flows over the network links.

Next, the effect of link removal on the active power flows over the remaining network links is calculated using (23). Fig. 2(a) illustrates how the flows over the network links are affected by a particular link removal, as compared to the previous flow over the removed link. As an example, when link 6 is removed from the network, due to the redistribution of power flow, the flows over links 4 and 7 increase by the amount of the previous flow over the removed link 6. Indeed, this makes the removal of link 6 critical. In order to avoid cascading failures, it must be checked whether the excess capacity of links 4 and 7 can handle the redistributed flow. For the network links 2, 3, and 5, the removal of link 6 decreases the flow over them, thus there is no possibility of cascading failure due to these links.

Finally, from (25), the effect of link additions is calculated and Fig. 2(b) displays some examples of the changes in the flows over the network links in case of a link addition, as compared to the flow over the added link. As expected, a link addition to the network mostly decreases the flows over the network links. For instance, when a new link is added between nodes 2 and 6, the flows over all network links decrease except for link 1, which is connected to the network as a branch. In addition, depending on the purpose of the new investment (link addition), Fig. 2(b) can be used to identify the place of the added link. For example, if the aim is to decrease the flow over link 5 between

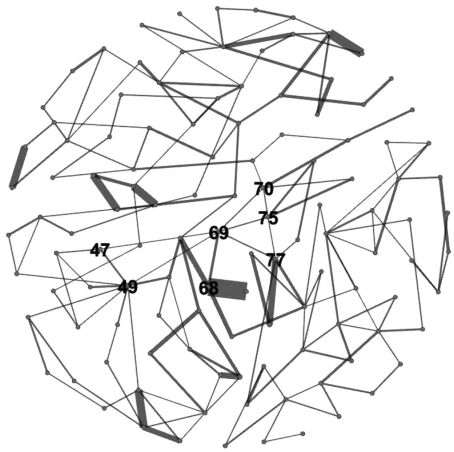


Fig. 3. Graph representation of the IEEE 118-buses power system. The thicknesses of the links represent the link weights, i.e., inverse of transmission line reactances. The average degree in the graph is 3.034, whereas the average weighted degree is 59.759. The network diameter is 14 and the average path length is 6.309. The links connected to node 69, an important generator bus serving 12% of the total demand, and their node pairs are chosen to be the observed set $(a, b)$.

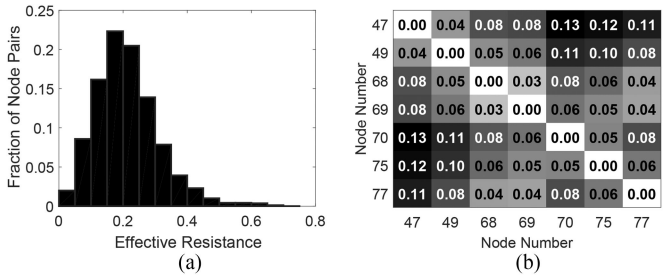


Fig. 4. Effective resistances in the IEEE 118-bus system. (a) All node pairs, and (b) Observed set.

nodes 3 and 4, three choices are effective: A new link parallel to link 5, a new link between nodes 3 and 5, or a new link between nodes 3 and 6 significantly decrease the flow, whereas the addition of a new link between nodes 1 and 5 has a relatively small effect on the observed link for the same amount of new flow. In some cases, the addition of new links can lead to an increase in the flow over a particular link. For instance, when a new link is added between nodes 3 and 6, the flow over link 2 increases considerably, which is the so-called Braess' paradox in power systems [27]. Therefore, such cases should be avoided or carefully investigated before realization.

### *B. IEEE 118-Bus Power System*

In this section, the realistic IEEE 118-bus power system is considered. Fig. 3 shows the graph representation of the network, containing in total 118 nodes and 179 links. The direction of existing flows over the links is defined according to initial conditions.

The histogram of effective resistances between all node pairs is shown in Fig. 4(a) and between the observed set in Fig. 4(b), respectively. The effective resistances in the observed set are relatively small, which indeed suggests a strong electrical

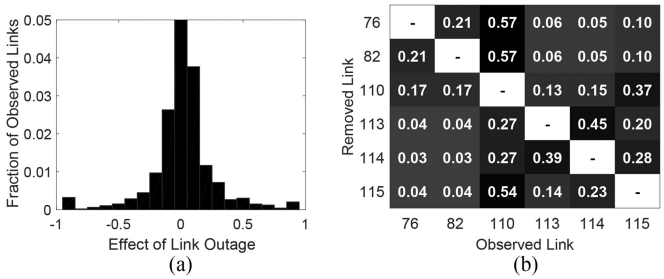


Fig. 5. Effect of link removal in the IEEE 118-bus system. In Fig. 5(a), the peak corresponding to $-0.05 \leq \frac{\Delta f_{ab}}{f_{ij}} \leq 0.05$ is 0.8327. (a) All cases, and (b) Observed set.

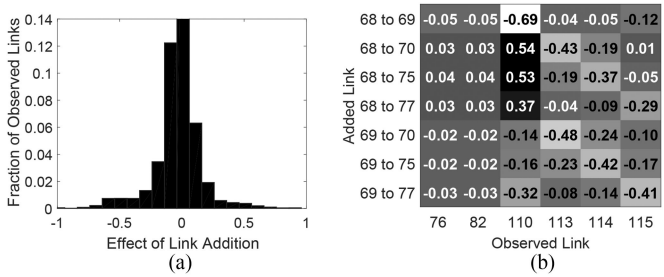


Fig. 6. Effect of link addition in the IEEE 118-bus system. In Fig. 6(a), the peak corresponding to $-0.05 \leq \frac{\Delta f_{ab}}{f_{ij}} \leq 0.05$ is 0.7035. (a) All cases, and (b) Observed set.

connection, whereas the larger values of effective resistances in Fig. 4(a) suggest the opposite, indicating the points with less back-up paths in the network.

The effect of each link removal on each remaining network link is calculated using (24) resulting in 179 link removal cases, each with 178 observed links. The histogram of the calculated effects of link removals relative to the flow over the removed link is shown in Fig. 5(a). Approximately 95% of the calculated effects have magnitude smaller than 0.2, which is a sign of a meshed network with alternative paths. However, in 3.8% of the calculated effects, (23) results in 0, which refers to network links which are connected as branches to the meshed part of the network.

In Fig. 5(a), 0.17% of the effects of the link removals have the value 1, meaning that the previous flow of the removed element is transferred to a single alternative path. From a robustness point of view, the less frequent this is, the more robust is the network against overloads due to link removals. Therefore, these cases should be analyzed in reliability assessments. Additionally, the removal of 9 links leads to isolation of one or more nodes in the network, which is again undesirable in a robust network.

In Fig. 5(b), the effect of link removals in the observed set is shown. When link 76, 82, or 115 is removed from the network, more than half of the redistributed flow goes through link 110 between nodes 68 and 69, which makes link 110 critical. As a remark, when a link is removed in the observed set, the magnitude of the changes in the flows over remaining links must sum up to the previous flow over the removed link according to Kirchhoff's law, therefore the row sums in Fig. 5(b) are all 1.

From (25), the effect of link addition between each node pair in the network is calculated, resulting in $\frac{118\times117}{2} = 6903$ link addition cases, each with 179 observed links. The histogram of the effects of all possible link additions relative to the flow over the added link is presented in Fig. 6(a). Of the calculated effects, 92% have magnitude smaller than 0.2, which again follows from the meshed structure and the existence of alternative paths for the redistributed power. Due to the meshed structure, a link addition to the network can increase the flows over the network links. However, the probability of an increase in magnitude is less than compared to the probability of a decrease, which can be observed from the asymmetrical distribution in Fig. 6(a).

In Fig. 6(b), the effect of link addition in the observed set is shown. Similar to the link removal case, when a link connected to node 69 is added, the observed relative changes in the magnitudes must sum up to 1. The magnitude of the flow over link 110 increases in 3 out of the 7 illustrated link additions, which urges detailed assessments before realization of these link additions in order to avoid Braess' paradox.

## V. Conclusion

This paper has provided an extended graph approach to analyze the physical operation and the vulnerability of an electrical grid from a topological point of view. Contrary to the representation in electrical engineering, the linearized power flow behaviour was expressed in terms of slack-bus independent graph-related matrices. Moreover, a closed formula for the effective resistance matrix, which combines the fundamentals of an electrical power grid with the topological structure, was proposed. The paper has further derived the expressions for the sensitivities of active power flows in link removal/addition cases to assess the topological vulnerability of a power grid. Consequently, link removals that may result in cascading failures or node isolation and link additions that decrease the critical flows or result in Braess' paradox in the power grid were identified.

## Appendix
## Power Flow Equations

The equations are derived for the power flow in a particular bus (node) $i$. The injected power $S_i$ at bus $i$ is defined as

$$S_i = V_i I_i^* \tag{31}$$

where $I_i^*$ is the complex conjugate of the current through bus $i$, and $V_i$ is the voltage at bus $i$. Kirchhoff's law expresses the current in terms of network voltage and admittance quantities:

$$S_i = V_i(\mathbf{YV})_i^* = V_i \sum_{k=1}^{N} Y_{ik}^* V_k^* \tag{32}$$

where $N$ is the number of buses in the system, $\mathbf{V} = [V_1 \dots V_N]^{\mathrm{T}}$ is the vector of bus voltages, and $\mathbf{Y}$ is the admittance matrix with entries

$$Y_{ik} = \begin{cases} y_{ii} + \sum_{i \neq k} y_{ik}, & \text{if } i = k \\ -y_{ik}, & \text{if } i \neq k \end{cases} \tag{33}$$

where $y_{ii}$ is the selfadmittance [20] of the bus and $y_{ik}$ is the equivalent admittance of all transmission adjacent lines from bus $i$ to $k$. If $y_{ii} = 0$ for each bus $i$, then an important feature of the admittance matrix $\mathbf{Y}$, that follows from the definition (33), is that the sum of the elements of a row equals zero:

$$\mathbf{Y}\,\mathbf{u} = \mathbf{0} \tag{34}$$

where the all-one vector $\mathbf{u} = [1 \dots 1]^{\mathrm{T}}$.

Equation (34) is a special case of an eigenvalue equation, illustrating that the all-one vector is an eigenvector belonging to eigenvalue zero. The latter also implies that the determinant of the admittance matrix $\mathbf{Y}$ is zero and, consequently, that the inverse of $\mathbf{Y}$ does not exist.

Introducing the phasor representation [20] of voltage into (32), and rewriting the elements of the admittance matrix as $Y_{ik} = G_{ik} + \iota B_{ik}$ lead to

$$S_i = \sum_{k=1}^{N} |V_i||V_k|(\cos\theta_{ik} + \iota \sin\theta_{ik})(G_{ik} - \iota B_{ik}) \tag{35}$$

where $\theta_{ik} = \theta_i - \theta_k$. Using the definition of complex power, $S_i = P_i + \iota Q_i$, yields

$$P_i = \sum_{k=1}^{N} |V_i||V_k|(G_{ik}\cos\theta_{ik} + B_{ik}\sin\theta_{ik}) \tag{36}$$

$$Q_i = \sum_{k=1}^{N} |V_i||V_k|(G_{ik}\sin\theta_{ik} - B_{ik}\cos\theta_{ik}). \tag{37}$$

Equations (36) and (37), which relate voltages and power, are called the ac power flow equations.

### A. Solving the Power Flow Equations

Using (36) and (37), the aim is to calculate the unknown electrical properties of each bus in the power system assuming knowledge of:

1) the admittance matrix $\mathbf{Y}$;
2) the magnitude $|V_i|$ of voltage phasor of the slack-bus and the generator buses;
3) the real power injection $P_i$ of all buses except for the slack-bus;
4) the reactive power injection $Q_i$ of all load buses.

Given the above information, the aim is to find:

1) the angles $\theta_i$ of the voltage phasors at all buses, except for the slack-bus whose voltage phase angle is set to 0;
2) the magnitudes for the voltage phasors $|V_i|$ at all load buses.

There are several different methods to solve the nonlinear ac power flow (36) and (37). The most popular is the Newton Raphson method [20].

### B. DC Load Flow

The ac power flow equations are nonlinear and the solution process is generally iterative. A linear set of equations is more desirable whenever fast and repetitive solutions are needed. Linearization can be reasonably accurate when the following conditions are met [16].

1) The difference between the voltage phase angles of two neighbouring buses is small so that $\sin\theta_{ik} \simeq \theta_{ik}$ and $\cos\theta_{ik} \simeq 1$.
2) Line resistances $r_{ik}$ compared to the line reactances $x_{ik}$ are negligible, which causes the entries of the admittance matrix in (33) to be equal to the reciprocal of line reactance values, $b_{ik}$.
3) The variations in the bus voltage magnitudes are so small that they are assumed to be all equal to the selected system base.
4) Reactive power flows are negligible for each bus $i$.

If these conditions are met, in per unit system [20], (36) can be simplified to the so-called the dc load flow equation

$$P_i = \sum_{k=1}^{N} b_{ik}(\theta_i - \theta_k) \tag{38}$$

or, in matrix form using (33)

$$\mathbf{P} = \mathbf{Y}\boldsymbol{\Theta} \tag{39}$$

where $\mathbf{P} = [P_1 \dots P_N]^{\mathrm{T}}$ and $\boldsymbol{\Theta} = [\theta_1 \dots \theta_N]^{\mathrm{T}}$.

Since (34) implies that $\mathbf{Y}$ is not invertible, (39) cannot be directly solved as $\boldsymbol{\Theta} = \mathbf{Y}^{-1}\mathbf{P}$. The common procedure is to select a bus $i$ as a reference bus (slack-bus), and drop the equation corresponding to its power injection. Then, the remaining equations of bus voltage angles can be solved uniquely with respect to the slack-bus.

Obviously, a dc load flow solution is less accurate than an ac load flow solution. In transmission systems, the difference between voltage phase angles of neighbouring buses $\theta_{ik}$ is relatively small, thus the error is assumed to be negligible [16].

## REFERENCES


[1] R. Baldick *et al.*, "Initial review of methods for cascading failure analysis in electric power transmission systems," in *Proc. IEEE Power Eng. Soc. Gen. Meet.*, 2008, pp. 1–8.

[2] F. Alvarado and S. Oren, "Transmission system operation and interconnection," Nat. Transmission Grid Study, U.S. Dept. Energy, Washington, DC, USA, Tech. Rep., pp. A1–A35, 2002, Available: Online. http://www.kves.uniza.sk/kvesnew/dokumenty/EEAJ/T3_3_TS_operation.pdf

[3] S. H. Strogatz, "Exploring complex networks," *Nature*, vol. 410, pp. 268–276, 2001.

[4] A. -L. Barabasi and R. Albert, "Emergence of scaling in random networks," *Science*, vol. 286, pp. 509–512, 1999.

[5] P. Crucitti, V. Latora, and M. Marchiori, "A topological analysis of the Italian electric power grid," *Physica A*, vol. 338, pp. 92–97, 2004.

[6] E. Bompard, M. Masera, R. Napoli, and F. Xue, "Assessment of structural vulnerability for power grids by network performance based on complex networks," in *Critical Information Infrastructure Security*. New york, NY, USA: Springer,2009, pp. 144–154.

[7] E. Negeri, F. Kuipers, and N. Baken, "Assessing the topological structure of a smart low-voltage grid," *Int. J. Crit. Infrastruct. Prot.*, vol. 9, pp. 24–37, 2015.

[8] Y. Koc, M. Warnier, R. E. Kooij, and F. M. T. Brazier, "Structural vulnerability assessment of electric power grids," in *Proc. 11th IEEE Int. Conf. Netw., Sens. Control*, 2014, pp. 386–391.

[9] J. M. Hernandez and P. Van Mieghem, "Classification of graph metrics," *Delft Univ. Technol.*, Delft, The Netherlands, Tech. Rep. 20111111, 2011.

[10] M. Rosas-Casals, S. Valverde, and R. V. Sole, "Topological vulnerability of the European power grid under errors and attacks," *Chaos*, vol. 17, pp. 2465–2475, 2007.

[11] D. P. Chassin and C. Posse, "Evaluating North American electric grid reliability using the Barabasi-Albert network model," *Physica A*, vol. 355, pp. 667–677, 2005.
[12] Y. Koc, M. Warnier, P. Van Mieghem, R. E. Kooij, and F. M. T. Brazier, "The impact of the topology on cascading failures in a power grid model," *Physica A*, vol. 402, pp. 169–179, 2014.
[13] X. Chen, K. Sun, Y. Cao, and S. Wang, "Identification of vulnerable lines in power grid based on complex network theory," in *Proc. Power Eng. Soc. Gen. Meet.*, 2007, pp. 1–6.
[14] E. Bompard, E. Pons, and D. Wu, "Extended topological metrics for the analysis of power grid vulnerability," *IEEE Syst. J.*, vol. 6, no. 3, pp. 481–487, Sep. 2012.
[15] S. Soltan, D. Mazauric, and G. Zussman, "Cascading failures in power grids analysis and algorithms," in *Proc. ACM Special Interest Group Data Commun. e-Energy*, 2014, pp. 195–206.
[16] D. Van Hertem, J. Verboomen, K. Purchala, R. Belmans, and W. Kling, "Usefulness of DC power flow for active power flow analysis with flow controlling devices," in *Proc. AC DC Power Transmiss.*, 2006, pp. 58–62.
[17] P. Van Mieghem, *Graph Spectra for Complex Networks*. Cambridge, Cambridge, U.K.: Cambridge Univ. Press, 2011.
[18] W. Ellens, F. M. Spieksma, P. Van Mieghem, A. Jamakovic, and R. E. Kooij, "Effective graph resistance," *Linear Algebra Appl.*, vol. 435, pp. 2491–2506, 2011.
[19] K. Purchala, L. Meeus, D. Van Dommelen, and R. Belmans, "Usefulness of DC power flow for active power flow analysis," in *Proc. Power Eng. Soc. Gen. Meet.*, 2005, pp. 454–459.
[20] J. J. Grainger and W. D. Stevenson, *Power System Analysis*. New York, NY, USA: McGraw-Hill, 1994.
[21] A. Ghosh, S. Boyd, and A. Saber, "Minimizing effective resistance of a graph," *SIAM Rev.*, vol. 50, pp. 37–66, 2008.
[22] T. Guler, G. Gross, and M. Liu, "Generalized line outage distribution factors," *IEEE Trans. Power Syst.*, vol. 22, no. 2, pp. 879–881, May 2007.
[23] J. Guo, Y. Fu, Z. Li, and M. Shahidehpour, "Direct calculation of line outage distribution factors," *IEEE Trans. Power Syst.*, vol. 24, no. 3, pp. 1633–1634, Aug. 2009.
[24] P. W. Sauer, K. E. Reinhard, and T. J. Overbye, "Extended factors for linear contingency analysis," in *Proc. 34th Hawaii Int. Conf. Syst. Sci.*, 2001, pp. 697–703.
[25] C. D. Meyer, Jr., "Generalized inversion of modified matrices, *" SIAM J. Appl. Math.*, vol. 24, pp. 315–323, 1973.
[26] L. O. Chua, C. A. Desoer, and E. S. Kuh, *Linear and Nonlinear Circuits*. New York, NY, USA: McGraw-Hill, 1987.
[27] X. Wang, Y. Koc, R. E. Kooij, and P. Van Mieghem, "A network approach for power grid robustness against cascading failures," in *Proc. 7th Int. Workshop Reliable Netw. Des. Model.*, 2015, pp. 1–8.

**Hale Cetinay** received the B.Sc. degree and the M.Sc. degree in electrical and electronics engineering from the Middle East Technical University, Ankara, Turkey, in 2011 and 2014, respectively. She is currently working toward the Ph.D. degree since September 2014 at Delft University of Technology, Delft, The Netherlands.

Her main research interests include network science, electrical networks, and smart grids.

**Fernando A. Kuipers** (SM'10) received the Ph.D. degree *cum laude* (highest distinction) from the Delft University of Technology (TUDelft), Delft, The Netherlands, in 2004.

He is currently an Associate Professor working on internet science at TUDelft. He was a Visiting Scholar at Columbia University in 2016 and Technion in 2009. His research focus is on network optimization, network resilience, quality of service, and quality of experience and addresses problems in software-defined networking, optical networking, content distribution, and cyber-physical systems/infrastructures. His work on these subjects include distinguished papers at the IEEE International Conference on Computer Communications 2003, Chinacom 2006, IFIP Networking 2008, IEEE Future Multimedia Networking 2008, IEEE International Symposium on Multimedia 2008, International Test Conference 2009, IEEE Intelligence and Security Informatics Conference 2014, and NetGames 2015.

Dr. Kuipers is a Member of the Executive Committee of the IEEE Benelux Chapter on Communications and Vehicular Technology.

**Piet Van Mieghem** received the Master's (*magna cum laude*) and Ph.D. (*summa cum laude*) degrees in electrical engineering from the K.U. Leuven, Leuven, Belgium, in 1987 and 1991, respectively.

Since 1998, he has been working as a Professor with Delft University of Technology, Delft, The Netherlands, and the Chairman of the section Network Architectures and Services. His main research interests include modeling and analysis of complex networks and in new Internet-like architectures and algorithms for future communications networks. Before joining the Delft University of Technology, he worked at the Interuniversity Micro Electronic Center from 1987 to 1991. During 1993–1998, he was a Member of the Alcatel Corporate Research Center, Antwerp, Belgium. He was a Visiting Scientist at Massachusetts Institute of Technology (1992–1993), a Visiting Professor at the University of California at Los Angeles (2005), a Visiting Professor at Cornell University (2009), and at Stanford University (2015). He authored *Performance Analysis of Communications Networks and Systems* (Cambridge Univ. Press, 2006), *Data Communications Networking* (Techne, 2011), *Graph Spectra for Complex Networks* (Cambridge Univ. Press, 2011), and *Performance Analysis of Complex Networks and Systems* (Cambridge Univ. Press, 2014). He was a Member of the Editorial Board of *Computer Networks* (2005–2006), the IEEE/ACM TRANSACTIONS ON NETWORKING (2008–2012), and the *Journal of Discrete Mathematics* (2012–2014), and *Computer Communications* (2012–2015). Currently, he serves on the Editorial Board of the OUP *Journal of Complex Networks* since its launch in 2012.